CARBON 86 (2015) 132–138

Available at www.sciencedirect.com

ScienceDirect

journal homepage: www.elsevier.com/locate/carbon

Effects of molecular structures of carbon-based molecules on bio-lubrication

Yan Zhou [a], Jeremy Dahl [b], Robert Carlson [b], Hong Liang [a,c,*]

[a] Materials Science and Engineering, Texas A&M University, TX 77843, United States
[b] Stanford Institute for Materials & Energy Sciences, Stanford University, Menlo Park, CA 94025, United States
[c] Mechanical Engineering, Texas A&M University, College Station, TX 77843, United States

ARTICLE INFO

Article history:
Received 27 September 2014
Accepted 10 January 2015
Available online 19 January 2015

ABSTRACT

The lack of lubrication affects the performance of both natural and artificial joints and often leads to their failure. This research investigates the tribological performance of four carbon-based molecules, phloroglucinol, 1,2-dihydroxynaphthalene, graphene oxide (GO), and diamondoid (diamantane-4,9-dicarboxylic acid), as water-based lubricants against ultra-high-molecular-weight polyethylene (UHMWPE). Results showed friction reduction for all lubricants and GO performed the best. Molecular dynamics simulations indicated that GO flakes were prone to be adsorbed on the surface. The mending effect was dominant for the rest molecules that is less effective in lowering friction.

1. Introduction

Synovial joints present extremely low friction coefficients (0.003) with a lifespan for more than 70 years [1–5]. The lubrication in synovial joints is a complex process possessing multi-mechanisms including boundary lubrication [5–8], hydrodynamic and elastrohydrodynamic lubrication [9,10], and mixed lubrication [2]. According to the American Academy of Orthopaedic Surgeons, there are 543,000 total knee replacements performed per year in U.S. alone [11]. The life expectancy of current prosthetic implant is limited to 10–15 years [12]. In natural joints, articular cartilages slide against each other in a cavity filled with synovial fluid. The lack of lubrication affects the performance of both natural and artificial joints and often leads to their failure [13,14]. In patients undergoing arthroplasty, the synovial membrane that produces lubricant hyaluronan is reformed, causing a reduction in secretion [15]. Hyaluronan has been used as an intra-articular injection agent in order to relieve pains in patients with osteoarthritis, but beneficial effects are debated [16–19] that is probably due to the bio-degradation of hyaluronan and the lack of a continuous supplying method. It is of interest to search for lubricants that are effective and compatible with the surface materials of artificial joints.

Carbon-based lubricant molecules have been studied and applied in lubrication, such as carbon nanotube, graphene, graphene oxide (GO), graphite, fullerene, and diamondoid. Graphene is a 2D sheet of graphite that has a single atomic layer of carbon atoms [20]. Favorable properties of graphene include: extreme mechanical stiffness, elasticity and strength, high electrical and thermal conductivity, gas impermeability, and many others [21,22]. The oxidation products of graphene, GO, present hydroxyl groups, carboxyl groups, and others on the 2D plane, though certain bonds are disrupted by the oxidation process. Graphene and GO have been applied as single- or multi-layer coatings on sliding surfaces in order to

* *Corresponding author at:* Mechanical Engineering, Texas A&M University, College Station, TX 77843, United States.
E-mail address: hliang@tamu.edu (H. Liang).
http://dx.doi.org/10.1016/j.carbon.2015.01.017
0008-6223/

reduce wear and friction. In addition, graphene has been used as an additive in oil or organic solvent to provide lubrication. The large van der Waals forces between graphene flakes results in their aggregations in water and limits the possibility of use as a water-based lubricant without adding surfactants [23], which are usually harmful for biomedical applications. The oxidative functional groups make GO flakes hydrophilic so that water molecules are able to intercalate [24]. GO flakes can be dispersed easily in water and were shown as effective water additives [25,26]. Diamantane is a member of the diamondoid molecular series [27,28]. Diamondoids are composed of sp^3 carbon atoms arranged in the 3D carbon framework of diamond: its structure can be superimposed upon the diamond lattice. Diamantane is the 2-diamond-crystal cage member of the nanodiamond, diamondoid series. The one-cage member, the smallest diamondoid, is adamantane, a compound whose derivatives are used in pharmaceuticals that treat viral infections and neurological disorders [29], in the synthesis of high-temperature polymers, and many other applications [27,28]. Alkylated diamondoids and adamantane diesters have been used in various synthetic lubricants [30,31], but no report has been found on the biological lubricants. Diamondoids with more than three cages, known as the "higher diamondoids,"[32] have recently become available and shown to have many unusual and useful properties [33,34]. Like graphene, underivatized diamantane is strongly hydrophobic and aggregations in aqueous solutions [35]. Accordingly, the more hydrophilic derivative, diamantane-4,9-dicarboxylic acid (4,9D) [36] was applied in these studies.

The relationship between the molecular structures and the bio-tribological performance of the carbon-based lubricants is of great interest and is expected to guide further development and optimization of bio-lubricants in artificial joints. In this research, the carbon-based molecules of various dimensional and geometrical complexities–phloroglucinol (phl), 1,2-dihydroxynaphthalene (dhn), GO, and 4,9D–were studied for their bio-tribological behaviors on a common artificial joint material, ultra-high-molecular-weight polyethylene (UHMWPE). Molecular dynamics simulations were carried out to provide molecular level understanding in the interactions between the lubricants and the polymeric surfaces. The locations and kinetics during the adsorption of lubricants were determined.

2. Materials and methods

2.1. Materials

Four types of carbon-based molecules were investigated: phloroglucinol (phl), 1,2-dihydroxynaphthalene (dhn), diamantane-4,9-dicarboxylic acid (4,9D) [36], and graphene oxide (GO). Fig. 1 shows the structures of phl, dhn, and 4,9D. For phl, three hydroxyl groups are connected to one ring. For dhn, two hydroxyl groups are synthesized on the naphthalene structure. Both phl and dhn were obtained from Sigma–Aldrich.

GO was fabricated using improved Hummers method [37,38]. In brief, 60 ml H_2SO_4 was mixed with 6.7 ml H_3PO_4 and the mixed solution was added to a mixture of 0.5 g graphite powder (Sigma–Aldrich) and 3.0 g $KMnO_4$. The mixture was then heated in a water bath at 50 °C while stirred for 12 h. The resulting product was added to ice made from 66.7 ml H_2O and 0.5 ml H_2O_2. The solution was filtered using a paper filter. The filtrate was rinsed and centrifuged with 10% HCl three times (600 ml total), then DI water three times (600 ml total). Lastly, it was dried under vacuum at room temperature and the washed GO was weighed and re-dispersed in water. The GO-containing water solution was dried on a Si substrate for atomic force microscope (AFM) imaging, as seen in Fig. 2. The micron-sized GO flakes showed a height profile of ~1 nm that corresponds to a single-layered structure [24,39]. All lubricants were in 0.4 mg/ml water solution for tribo-testing.

2.2. Tribological characterization

A tribometer (Model TRB, CSM Instruments Inc., Switzerland) was used in the study of the frictional behaviors. A pin-on-disc arrangement was applied with a glass ball of 6.35 mm diameter as the pin and a UHMWPE disc. The testing speed was 1.5 cm/s and the normal load was 1 N. 50 cycles were tested [40,41].

2.3. Molecular dynamics simulation

Materials Studio 6.0 (Accelrys, San Diego) was used to perform the molecular dynamics (MD) simulation. The structures of lubricants were constructed and their geometries were

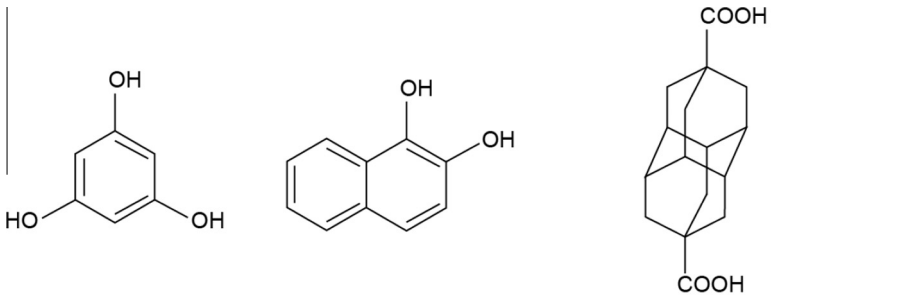

Fig. 1 – Molecular structures of phl, dhn, and 4,9D.

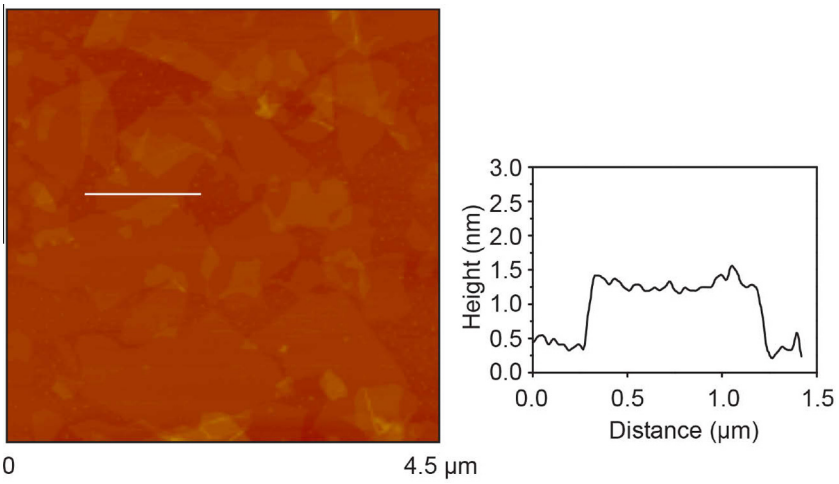

Fig. 2 – AFM image of GO flakes after drying on a Si substrate. The image was taken under non-contact mode. The plot on the right represents the height profile. (A colour version of this figure can be viewed online.)

optimized. According to Shih et al. [42], the formula of GO was set to as $C_{10}O_1(OH)_1(COOH)_{0.5}$ and the dimension of a GO flake was 10×10 Å. The surface of amorphous UHMWPE was constructed according to Liu et al. [43]. Using Amorphous Cell, the polymer molecules of 15 repeating units were packed in a confined layer to reach the density of UHMWPE at 0.94 g/cm^3. Two layers of xenon crystals were used as bottom and top walls. The hypothetical structure of the xenon crystal provided a flat surface with inert atoms that are suitable for acting as confining walls. Dynamics equilibration was applied to relax the system. After the removal of the xenon layers, the equilibrated confined layer of polyethylene was achieved. Super layers of several unit cells were built along the *xy* plane. Fig. 3 shows a layer of 4 unit layers with a dimension of $40 \times 40 \times 26$ Å, in which the *xy* plane was the surface used.

The kinetics of the adsorption in water were studied using the Forcite module with the dynamics task, where the atoms of the surface were fixed. A box of $40 \times 40 \times 30$ Å was constructed that filled with water and lubricant molecules. The box was placed on top of the surface super layer and below a vacuum layer of 70 Å. NVT assembly and a total of 20 ps were used. The Adsorption Locator module was applied to determine the locations of the adsorbed lubricants, where COMPASS force field was in use and no water molecules was included.

3. Results and discussion

3.1. *Tribological performance*

The four tested potential bio-lubricants share two similarities: (a) a ring of 6 carbon as the building block; (b) OH and/or COOH functional groups for improved water solubility. Fig. 4 shows the coefficient of friction (COF) of non-additized

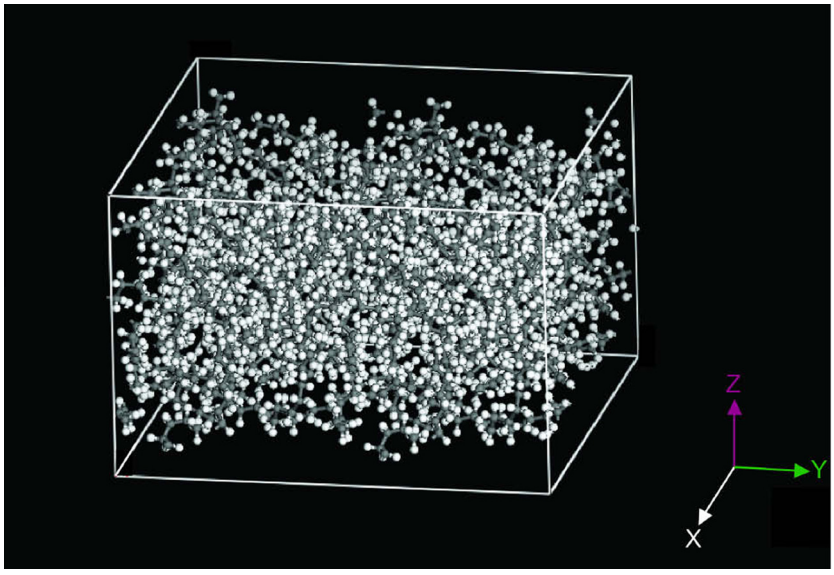

Fig. 3 – The amorphous cell of polyethylene of 4 units. The dimension is $40 \times 40 \times 26$ Å. (A colour version of this figure can be viewed online.)

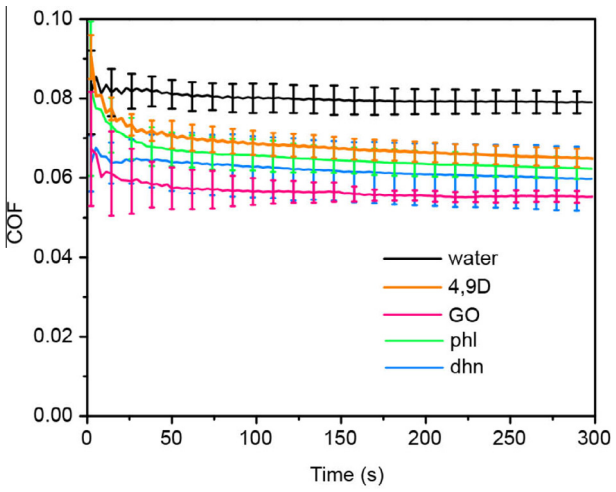

Fig. 4 – COFs of water, 4,9D, GO, phl, and dhn. (A colour version of this figure can be viewed online.)

Table 1 – Surface roughness of the simulated UHMWPE surface.

Roughness parameters	Values (Å)
Ra	1.05 ± 0.22
Rz	4.09 ± 0.59
Rq	1.27 ± 0.26
Rt	5.26 ± 0.37

lubrication (water only) was around 0.08. The addition of carbon-based lubricants reduced COFs. 4,9D lowered the COF but was less effective compared with GO, phl, and dhn. The GO appeared to be the best water-based lubricant under testing conditions and reduced the COF to below 0.06. The COF of dhn was ~0.02 lower than that of water. The results indicate the tested carbon-based lubricants could improve UHMWPE's lubricating ability.

The friction reduction trend is: GO > dhn > phl > 4,9D > water. As the best lubricant, the 2D GO flakes are micron-sized, which are larger than dhn, phl, and 4,9D. 4,9D is the only 3D lubricant and the least effective one in friction reduction. Phl and dhn are composed of 1 and 2 building blocks and their lubricating performances were between GO and 4,9D. The frictional tests are designed to be in the boundary lubrication regime where the surface adsorption of lubricants plays a major role in friction. For 3D lubricants, such as nanoparticles, the friction reduction mechanisms include ball-bearing effect [44–47], mending effect (filling in surface valleys) [48], protective layer [49], and polishing effect [50]. Kinoshita et al. showed that the 2D GO sheets in water reduced boundary friction through surface adsorption and the formation of a protective layer [25]. Hence, MD simulations were applied to explore the surface adsorption.

3.2. *Surface adsorption*

The roughness parameters of the simulated UHMWPE surface were calculated (Table 1). The Ra values of the simulated surface and the experiential surface are 1.05 ± 0.22 Å and 0.436 ± 0.072 μm, respectively. Except GO, the sizes of phl, dhn, and 4,9D are less than 1 nm. Hence, the nanoscale surface roughness is more meaningful in studying the adsorption of lubricants and was calculated based on the 4 × 4 nm unit cell generated in Materials Studio.

The kinetics of the adsorption of lubricants in water was examined. In Fig. 5(a), the distances between the lubricant molecules and the polymeric surface were expressed as functions of the simulation time. Fig. 5(b) shows the constructed lubricant-water-polymer system. Except for GO, the lubricants either approached the surface (solid symbols) or idled above (hollowed symbols). Initially, all lubricants idle in the

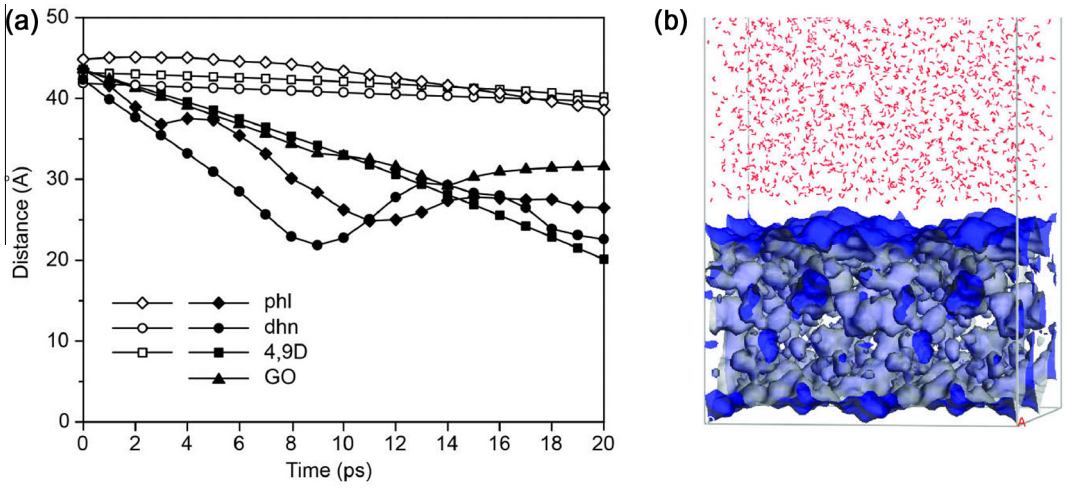

Fig. 5 – The kinetics of lubricant adsorption in a water environment. (a) Distance between the lubricants and the polymeric surface in 20 ps (solid: molecules approach the surface; hollow: molecules idle above the surface). (b) The system constructed for the kinetics simulation. Water box atop a polymer box with red dots as water. (A colour version of this figure can be viewed online.)

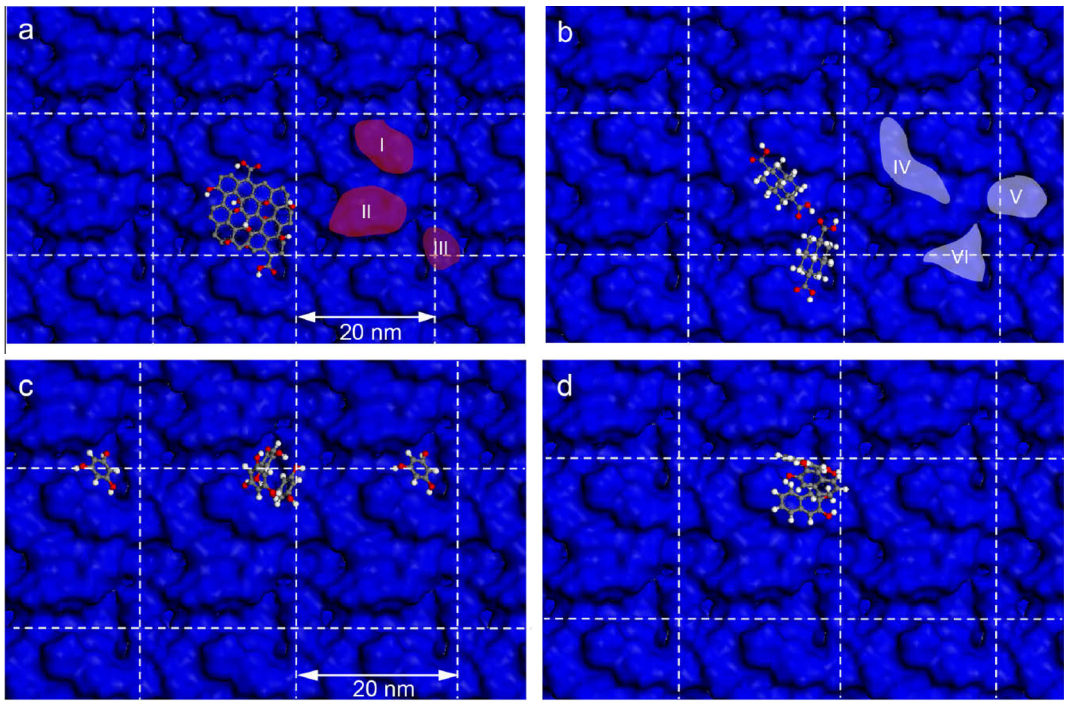

Fig. 6 – The locations of surface adsorption of (a) GO, (b) 4,9D, (c) phl, and (d) dhn. The dashed lines separate the repeating units. Shadowed area I–III are the peaks; shadowed area IV–VI are the valleys. (A colour version of this figure can be viewed online.)

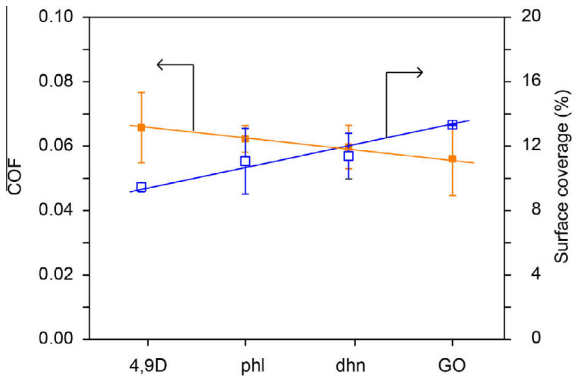

Fig. 7 – The COFs (solid square; based on results in Fig. 4) and surface coverage from the simulation (hollow squares) of 4,9D, phl, dhn, and GO. Linear trend lines added. (A colour version of this figure can be viewed online.)

water environment. As a result of Brownian motion, some lubricants approach the surface and then the strong attractive forces (van der Waals and electrostatic) between the surface and the lubricants keep lubricants being adsorbed. For small molecules (phl, dhn, and 4,9D), Brownian motion is strong that overwhelms the attractive forces, resulting more idling molecules. For big molecules (GO), the attractive forces suppress Brownian motion, resulting only adsorption.

Fig. 6 shows the adsorbed lubricants on the polymeric surface with the dashed lines as the boundaries of repeating units. In order to achieve a same concentration, 1 GO molecule, 5 phl molecules, 4 dhn molecules, and 2 4,9D molecules were used in the simulation, respectively. The shadowed areas I–III and IV–VI indicate peaks and valleys on the surface, respectively. In Fig. 6(a), as expected, the peaks were covered by GO: II was fully covered and I and III were partially covered. In Fig. 6(b), due to the smaller size and geometry, 4,9D molecules were all trapped in the valleys on the surface: IV and VI were filled each with 1 4,9D molecule. In Fig. 6(c), either 3 phl molecules stacked or 1 phl molecule in valley VI. Fig. 6(d) shows 1 dhn molecule on peak I and 2 dhn molecules in valley VI.

The surface coverage by lubricant molecules was calculated and plotted together with their experimental COFs in Fig. 7. The COFs from the lubricants decrease with the increase of their surface coverage. 4,9D showed the highest COF and the lowest surface coverage at 9.46%. This phenomenon corresponds to the mending effect that 4,9D molecules were trapped in the valleys. The simulated GO flakes showed the highest surface coverage (13.33%) and the lowest experimental COF. The size of the simulated GO flakes (10×10 Å) was much smaller than that in experiments (see Fig. 2). The real surface coverage would be significantly higher. Phl and dhn shared similar surface coverage and COF.

Fig. 8 presents the proposed mechanism. The friction is reduced when the lubricant molecules cover nanoscale peaks ($l > s$) hence keep the asperities from adhering, where a protective layer formed. For smaller lubricants ($d < s$), the peaks are covered less since lubricant molecules trap in the valleys (mending effect). The numbers of carbon atoms per unit cell are 6, 5, and 2 for phl, dhn and GO, respectively. At the same weight concentration, GO provides the most unit cells while phl the least. Large molecules are prone to be adsorbed but small ones idle above the surface.

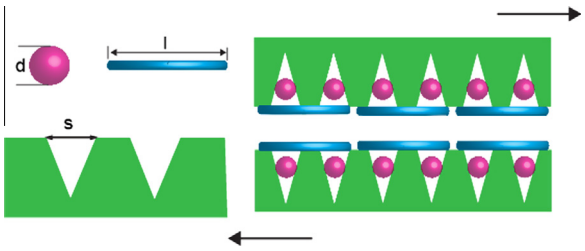

Fig. 8 – Friction reduction mechanism based on the size of the carbon-based lubricants. GO flakes cover the nanoscale peaks and prevent adhesion. Small lubricant molecules trap in the valleys. (A colour version of this figure can be viewed online.)

4. Conclusions

In summary, the effects of molecular structures of carbon-based molecules as potential bio-lubricants have been studied. Phloroglucinol, 1,2-dihydroxynaphthalene, graphene oxide, and diamondoid were explored as water-based lubricants against common polymeric biomaterials of artificial joints. All tested lubricants reduced the friction on self-lubricating UHMWPE and the friction reduction trend is: graphene oxide > 1,2-dihydroxynaphthalene > phloroglucinol > diamondoid > water. Molecular dynamics simulations showed that graphene oxide flakes were prone to keep being adsorbed on the surface. The mending effect was dominant for phloroglucinol, 1,2-dihydroxynaphthalene, and diamondoid that was less effective in lowering friction than the protective layer formed by 2D graphene oxide. The revealed correlations between the dimensional complexities and the friction reduction mechanisms allow the development of lubricants for better performance in prosthesis.

Acknowledgments

Diamantane-4,9-dicarboxylate was generously provided by Prof. Peter R. Schreiner. The authors thank the Laboratory for Molecular Simulation at Texas A&M University for providing the software. Diamondoid isolation and derivatization was supported by the US Department of Energy, Office of Science, Basic Energy Sciences, Materials Sciences and Engineering Division, under contract DEAC02-76SF00515. Authors thank Xingliang He at Texas A&M University for assistance in AFM analysis.

REFERENCES

[1] Hunter W. Of the structure and diseases of articulating cartilages, by William Hunter, surgeon. Philos Trans 1742;42(462–471):514-21.
[2] Linn FC. Lubrication of animal joints: II the mechanism. J Biomech 1968;1(3):193–205.
[3] Wright V, Society BE. Lubrication and wear in joints. In: Proceedings of a symposium organized by the Biological Engineering Society, April 17 1969, The General Infirmary, Leeds. Lippincott; 1969.
[4] Wright V, Dowson D. Lubrication and cartilage. J Anat 1976;121(Feb):107–18.
[5] Hills BA. Oligolamellar lubrication of joints by surface-active phospholipid. J Rheumatol 1989;16(1):82–91.
[6] Rees SG, Davies JR, Tudor D, Flannery CR, Hughes CE, Dent CM, et al. Immunolocalisation and expression of proteoglycan 4 (cartilage superficial zone proteoglycan) in tendon. Matrix Biol 2002;21(7):593–602.
[7] Swann DA, Slayter HS, Silver FH. The molecular-structure of lubricating glycoprotein-i, the boundary lubricant for articular-cartilage. J Biol Chem 1981;256(11):5921–5.
[8] Murakami T, Higaki H, Sawae Y, Ohtsuki N, Moriyama S, Nakanishi Y. Adaptive multimode lubrication in natural synovial joints and artificial joints. Proc Inst Mech Eng [H] 1998;212(1):23–35.
[9] Dowson D. Paper 12: Modes of lubrication in human joints. In: Proceedings of the institution of mechanical engineers, conference proceedings: SAGE Publications; p. 45–54.
[10] Jin Z, Dowson D. Micro-elastohydrodynamic squeeze-film lubrication of compliant layered surfaces firmly bonded to a rigid substrate. Tribol Ser 1997;32:361–9.
[11] Hall MJ, DeFrances CJ, Williams SN, Golosinskiy A, Schwartzman A. National hospital discharge survey: 2007 summary. Natl Health Stat Rep 2010;29(29):1–20.
[12] Kutz M. Biomedical Engineering and Design Handbook. McGraw-Hill; 2009.
[13] Ahlroos T, Saikko V. Wear of prosthetic joint materials in various lubricants. Wear 1997;211(1):113–9.
[14] Yao JQ, Laurent MP, Johnson TS, Blanchard CR, Crowninshield RD. The influences of lubricant and material on polymer/CoCr sliding friction. Wear 2003;255(1–6):780–4.
[15] Mazzucco D, Scott R, Spector M. Composition of joint fluid in patients undergoing total knee replacement and revision arthroplasty: correlation with flow properties. Biomaterials 2004;25(18):4433–45.
[16] George E. Intra-articular hyaluronan treatment for osteoarthritis. Ann Rheum Dis 1998;57(11):637–40.
[17] Dougados M, Nguyen M, Listrat V, Amor B. High molecular weight sodium hyaluronate (hyalectin) in osteoarthritis of the knee: a 1 year placebo-controlled trial. Osteoarthritis Cartilage 1993;1(2):97–103.
[18] Listrat V, Ayral X, Patarnello F, Bonvarlet J-P, Simonnet J, Amor B, et al. Arthroscopic evaluation of potential structure modifying activity of hyaluronan (Hyalgan®) in osteoarthritis of the knee. Osteoarthritis Cartilage 1997;5(3):153–60.
[19] Altman RD, Moskowitz R. Intraarticular sodium hyaluronate (hyalgan) in the treatment of patients with osteoarthritis of the knee: a randomized clinical trial. Hyalgan Study Group. J Rheumatol 1998;25(11):2203–12.
[20] Novoselov K, Fal V, Colombo L, Gellert P, Schwab M, Kim K. A roadmap for graphene. Nature 2012;490(7419):192–200.
[21] Geim AK, Novoselov KS. The rise of graphene. Nat Mater 2007;6(3):183–91.
[22] Geim AK. Graphene: status and prospects. Science 2009;324(5934):1530–4.
[23] Shih CJ, Lin SC, Strano MS, Blankschtein D. Understanding the stabilization of liquid-phase-exfoliated graphene in polar solvents: molecular dynamics simulations and kinetic theory of colloid aggregation. J Am Chem Soc 2010;132(41):14638–48.
[24] Stankovich S, Dikin DA, Piner RD, Kohlhaas KA, Kleinhammes A, Jia Y, et al. Synthesis of graphene-based nanosheets via chemical reduction of exfoliated graphite oxide. Carbon 2007;45(7):1558–65.
[25] Kinoshita H, Nishina Y, Alias AA, Fujii M. Tribological properties of monolayer graphene oxide sheets as water-based lubricant additives. Carbon 2014;66:720–3.

[26] Song HJ, Li N. Frictional behavior of oxide graphene nanosheets as water-base lubricant additive. Appl Phys a-Mater 2011;105(4):827–32.
[27] Gunawan MA, Hierso JC, Poinsot D, Fokin AA, Fokina NA, Tkachenko BA, et al. Diamondoids: functionalization and subsequent applications of perfectly defined molecular cage hydrocarbons. New J Chem 2014;38(1):28–41.
[28] Schwertfeger H, Fokin AA, Schreiner PR. Diamonds are a chemist's best friend: diamondoid chemistry beyond adamantane. Angew Chem Int Ed 2008;47(6):1022–36.
[29] Wanka L, Iqbal K, Schreiner PR. The lipophilic bullet hits the targets: medicinal chemistry of adamantane derivatives. Chem Rev 2013;113(5):3516–604.
[30] Wu MM, Shen D-M, Chen CS, inventors; High viscosity index lubricant fluid. United States patent 5306851. 1994.
[31] Abraham S, Duling IN, inventors; Diesters containing adamantane nuclei. United States patent 3398165. 1968.
[32] Dahl JE, Liu SG, Carlson RMK. Isolation and structure of higher diamondoids, nanometer-sized diamond molecules. Science 2003;299(5603):96–9.
[33] Clay WA, Dahl JEP, Carlson RMK, Melosh NA, Shen Z-X. Physical properties of materials derived from diamondoid molecules. Rep Prog Phys 2014.
[34] Bostedt C, Landt L, Moller T, Dahl JE, Carlson RMK. Diamondoids. In: Barnard AS, Guo H, editors. Nature's nanostructures. Pan Stanford Publishing Pte., Ltd.; 2012. p. 169–94.
[35] Maciel C, Malaspina T, Fileti EE. Prediction of the hydration properties of diamondoids from free energy and potential of mean force calculations. J Phys Chem B 2012;116(45):13467–71.
[36] Fokina NA, Tkachenko BA, Dahl JEP, Carlson RMK, Fokin AA, Schreiner PR. Synthesis of diamondoid carboxylic acids. Synthesis-Stuttgart 2012;44(2):259–64.
[37] Marcano DC, Kosynkin DV, Berlin JM, Sinitskii A, Sun ZZ, Slesarev A, et al. Improved synthesis of graphene oxide. ACS Nano 2010;4(8):4806–14.
[38] Hummers WS, Offeman RE. Preparation of graphitic oxide. J Am Chem Soc 1958;80(6):1339.
[39] Stankovich S, Dikin DA, Dommett GHB, Kohlhaas KM, Zimney EJ, Stach EA, et al. Graphene-based composite materials. Nature 2006;442(7100):282–6.
[40] Ribeiro R. A tribological and biomimetic study of potential bone joint repair materials. Texas A&M University; 2006.
[41] Ribeiro R, Banda S, Ounaies Z, Ucisik H, Usta M, Liang H. A tribological and biomimetic study of PI–CNT composites for cartilage replacement. J Mater Sci 2012;47(2):649–58.
[42] Shih CJ, Lin SC, Sharma R, Strano MS, Blankschtein D. Understanding the pH-dependent behavior of graphene oxide aqueous solutions: a comparative experimental and molecular dynamics simulation study. Langmuir 2012;28(1):235–41.
[43] Liu HY, Li Y, Krause WE, Rojas OJ, Pasquinelli MA. The soft-confined method for creating molecular models of amorphous polymer surfaces. J Phys Chem B 2012;116(5):1570–8.
[44] Wu YY, Tsui WC, Liu TC. Experimental analysis of tribological properties of lubricating oils with nanoparticle additives. Wear 2007;262(7–8):819–25.
[45] Rapoport L, Leshchinsky V, Lvovsky M, Nepomnyashchy O, Volovik Y, Tenne R. Mechanism of friction of fullerenes. Ind Lubr Tribol 2002;54(4):171–6.
[46] Chinas-Castillo F, Spikes HA. Mechanism of action of colloidal solid dispersions. J Tribol T Asme 2003;125(3):552–7.
[47] Santos CM, Tria MCR, Vergara RAMV, Ahmed F, Advincula RC, Rodrigues DF. Antimicrobial graphene polymer (PVK-GO) nanocomposite films. Chem Commun 2011;47(31):8892–4.
[48] Liu G, Li X, Qin B, Xing D, Guo Y, Fan R. Investigation of the mending effect and mechanism of copper nano-particles on a tribologically stressed surface. Tribol Lett 2004;17(4):961–6.
[49] Hu ZS, Lai R, Lou F, Wang LG, Chen ZL, Chen GX, et al. Preparation and tribological properties of nanometer magnesium borate as lubricating oil additive. Wear 2002;252(5–6):370–4.
[50] Xu T, Zhao JZ, Xu K. The ball-bearing effect of diamond nanoparticles as an oil additive. J Phys D Appl Phys 1996;29(11):2932–7.